Hindawi
Polymer Crystallization
Volume 2023, Article ID 7454857, 10 pages
https://doi.org/10.1155/2023/7454857

Research Article

Nanolignin as Nucleating Agents Promoting Crystallization of Isotactic Polypropylene

Jing Chen,[1] **Tao Yang**,[2] **Yongchen Zhu**,[1] **Zhenyang Luo**,[1,3] **and Xiaofeng Ma**[1,3]

[1]*College of Science, Nanjing Forestry University, Nanjing 210037, China*
[2]*School of Chemistry and Chemical Engineering, Nanjing University of Science and Technology, Nanjing 210094, China*
[3]*Institute of Polymer Materials, Nanjing Forestry University, Nanjing 210037, China*

Correspondence should be addressed to Xiaofeng Ma; maxf@njfu.edu.cn

Received 9 August 2022; Revised 7 March 2023; Accepted 8 March 2023; Published 23 March 2023

Academic Editor: Dario Cavallo

Lignin is the second most abundant pollution-free biomass material. However, most of lignin is discarded as waste in river or burned as fuel, which results in serious environmental pollution problems and low utilization efficiency of lignin at present. Thus, high-value utilization of lignin has become a hot research field. Herein, nanolignin (nano-Lig) is prepared successfully by the self-assembly method, and then nano-Lig and isotactic polypropylene (iPP) are mixed to prepare a series of nano-Lig/iPP composites by the solution blending method. Nano-Lig not only enhance thermostability of iPP but also improve crystallization properties of iPP. When 1.0 wt% nano-Lig was added in iPP, the crystallinity of iPP increased by 6.39% compared to iPP. Nano-Lig can increase the crystallization rate of iPP through investigation of kinetics of nonisothermal crystallization, suggesting nano-Lig can be used as a nucleating agent for iPP.

1. Introduction

Isotactic polypropylene (iPP) is one of the most used, large volume, low price polymorphic semicrystalline thermoplastic polymers [1, 2]. It has several unique properties such as high toughness, elasticity, ease of processability, excellent water, and chemical resistance. Therefore, it can be found in various applications, such as the automobile industry, food packaging, and the manufacture of toys and furniture [3–6].

The fabrication of iPP products involves heating and cooling during processing. It melts and crystallizes upon heating and cooling, respectively. The ultimate properties of iPP products are mainly controlled by the polymer structure, which can be affected by these phenomena of melts and crystallizes during processing. iPP crystallizes into four forms, namely, monoclinic α, trigonal β, orthorhombic γ, and a mesomorphic form, under different thermal and mechanical conditions and the usage of nucleating agents (NAs) [7–12]. Different kinds of nucleating agents can affect not only the crystallization rate of iPP in the forming process but also the crystalline structure.

NAs can be divided into natural NAs, synthetic NAs, and inorganic NAs. The natural NAs mainly include rosin, sorbitol, and sorbitol derivatives such as dibenzylidene sorbitol and 3, 4-dimethyldibenzylidene sorbitol [13–24]. The synthetic NAs include polycyclic aromatic hydrocarbons, organic acids/salts, amides, [25] benzoic acid salts, [26] hydrazide compounds, [27] and various organic pigments. Inorganic NAs have various salts oxides, such as $CaCO_3$ [28, 29], talc [30, 31], and Al_2O_3 [32]. Three kinds of NAs can increase the rate of PP crystallization, and the temperature at which the maximum rate of crystallization occurs upon cooling from the molten state. However, the disadvantage of synthetic NAs is that the technology of their production is not environmentally friendly, which usually include several stages of organic syntheses using specialty compounds, as well as toxic solvents. Talc and other inorganic fillers are also suitable NAs; they are inexpensive and serve as reinforcing agents. However, high concentrations of these materials are needed.

Lignin is the second most abundant biopolymer on the earth next to cellulose and is obtained as a major industrial

waste material from pulp and paper industries [33]. Whereas 98% of the lignin is burned or discharged into rivers, thereby causing serious environmental pollution and grievous waste of renewable resources [34]. It has attracted much interest in scientific and industrial field because of its unique properties, such as environmentally friendly, sustainable, biodegradable, thermal stability, and low cost, which can contribute to the reduction of the environmental problem [35–41]. Thus, lignin has been applied to many fields, such as binder, carbon materials, fire retardant, and biomedical application [42–45]. In the past decades, nano-Lignin (nano-Lig) had been developed to design high-value materials. Nano-Lig has many merits, such as more uniform size, shape, and a high surface area to volume ratio, which helps to reinforce and strengthen polymer matrices and improve polymer thermal stability [46–48]. In addition, nano-Lig also shows superior dispersion and miscibility in the hydrophobic matrices [46]. The study of Nano-Lig mainly focus on lignin-based hydrogels [47] and enhancement mechanical properties of polyvinyl alcohol and polylactic acid [48]. However, to the best of our knowledge, there is still no report on using nano-Lig as NA for iPP, even though there was report on lignin could act as NA for iPP [49]. It is expected that nano-Lig can act as an effective NA for iPP; in other words, a smaller amount of nano-Lig can promote crystallization of iPP.

Herein, we report that nano-Lignin (nano-Lig) can serve as a NA for iPP. Nano-Lig is prepared by a simple self-assembly method using tetrahydrofuran as good solvent and H_2O as poor solvent. First, nano-Lig/iPP composites are prepared by the solution blending method. Second, the effect of nano-Lig on the melting properties, crystallization structure, and thermal stability of iPP are investigated. Finally, nonisothermal kinetics of crystallization of iPP and nano-Lig/iPP composite are demonstrated.

2. Experimental Section

2.1. Materials. iPP was purchased from Sinopec Yangzi Petrochemical Co., Ltd., China. Enzyme-hydrolyzed lignin was purchased from Shandong Longli Biotechnology Co., Ltd., China. Tetrahydrofuran (THF, AR, 99%) and xylene (AR, 99%) were purchased from Shanghai Macklin Biochemical Co., Ltd., China. Deionized water was obtained from Milli-Q.

2.2. Preparation of Nano-Lig. Nano-Lig aqueous solution was prepared by a simple self-assemble method according to a previous report [50]. The preparation process of nano-Lig was as follows (Scheme 1): enzyme-hydrolyzed lignin of 0.50 g was dissolved in 50 ml THF at room temperature. Then, deionized water of 200 mL was slowly dropped to the above lignin/THF solution under stirring. After dropping, the final solution was stirred for 4 h until the suspension was formed. Finally, the suspension was transferred into a dialysis bag (M_w: 14000) and dialyzed in deionized water. The water was changed every 6 h and repeated for 5 times to obtain nano-Lig aqueous solution. Nano-Lig powder was obtained after the vacuum freeze drying process of nano-Lig aqueous solution.

2.3. Preparation of Nano-Lig/iPP Composites. A series of nano-Lig/iPP composites (0.5 wt%, 1.0 wt%, 1.5 wt%, and 2.0 wt% nano-Lig) were prepared by the solution blend method. Here, we just show the preparation process of 1 wt% nano-Lig/iPP composite. 4.95 g iPP was dissolved in xylene at 130°C to obtain iPP/xylene solution. Then, nano-Lig of 0.05 g was added into iPP/xylene solution. After stirring and heating the solution at 80°C for 4 h, then the white nano-Lig/iPP composite was obtained after drying the solid product at 75°C under vacuum for 12 h.

2.4. Dynamic Light Scattering (DLS) Analysis. The diameter of nano-Lig in H_2O was determined by DLS analyzer (BIC-90plus PALS, Marven, England). About 1 mL nano-Lig aqueous solution was balanced for 5 min at room temperature before measurement, and the measurement result was the average of the 10 collected data.

2.5. Fourier Transform Attenuated Total Reflectance Infrared Spectroscopy (FTIR-ATR). The surface of the samples was scanned with FTIR-ATR. Each sample was scanned 32 times in the wavenumber range from 4000 cm^{-1} to 400 cm^{-1}.

2.6. X-Ray Diffraction (XRD) Analysis. The iPP and nano-Lig/iPP composites were crystallized at 120°C for 2 h, and then those samples were measured by X-ray diffractometer (D/Max 2500, Japan Science Co., Ltd.) to determine the crystal structure of iPP. The current of the instrument was 200 mA, the acceleration voltage of the instrument was 40 kV, $\lambda = 0.154$ nm, the scanning step was 0.02°, the range was 10°~25°, and the scanning step frequency was 2°/min.

2.7. Differential Scanning Calorimeter (DSC) Analysis. The crystallization and melting behavior of iPP and nano-Lig/iPP composites were studied by DSC (NETZSCHTG 214). The test atmosphere was N_2 and the sample was weighed about 3 mg. The testing process is as follows: Heating up to 200°C at a heating rate of 30.0°C min^{-1}, eliminating thermal history at 200°C for 1 min, cooling to 30°C at a cooling speed of 20°C min^{-1} at 30°C for 1 min, and then heating up (second heating) to 200°C at a heating rate of 20.0°C min^{-1}. The enthalpy of crystallization during the cooling process and the melting enthalpy during the second heating process were recorded. The crystallization peak temperature and melting temperature of the sample were obtained from the crystallization and melting curve, respectively. According to the assumption of the two-phase model, when the polymer is melted, only the crystal part of the polymer changes; so, the melting heat is essentially the heat needed to destroy the crystal structure. Thus, the higher the crystallinity is, the larger the melting heat is. In other words, the melting heat of the polymer is proportional to its

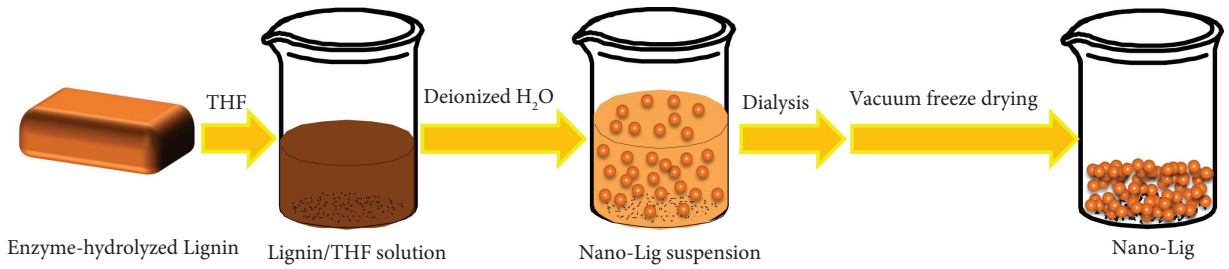

Scheme 1: Schematic illustration of the preparation of nano-Lig.

crystallinity. Using this principle, the crystallinity X_c of the polymer can be calculated by equation (1):

$$X_c = \frac{\Delta H}{\Delta H_0\left(1 - w_f\right)}, \quad (1)$$

where ΔH and ΔH_0 (207 J·g^{-1}) [51] are the heats of fusion of the experimental sample and the perfect (defect-free) iPP crystal, respectively. The w_f is the weight fraction of nano-Lig in the composite.

Nonisothermal kinetic test: the sample was heated to 200°C at a heating rate of 30.0°C min^{-1}. After the heat history was eliminated at 200°C for 1 min, it was cooled to 50°C at the cooling rates of 2.5°C min^{-1}, 5.0°C min^{-1}, 10.0°C min^{-1}, and 20.0°C min^{-1}, respectively. The crystallization curve and crystallization peak temperature at each cooling rate were recorded.

2.8. Thermogravimetric (TG) Analysis. Under N_2 atmosphere, the sample of 3 mg was weighed, the temperature increased from room temperature to 600°C at a heating rate of 20.0°C min^{-1}, and the mass change of the sample during the test was recorded.

3. Results and Discussion

3.1. Characterization of Nano-Lig and Nano-Lig/iPP Composites. Figure 1(a) shows the nano-Lig particle size distribution in H_2O at room temperature. The average particle size (hydrodynamic radius) of nano-Lig in H_2O was 153.2 nm, the particle size distribution (PDI) was 0.200, and the PDI was relatively narrow. Such size of nano-Lig is comparable with that of the previous report [50]. This result indicated that nano-Lig was prepared successfully. The FTIR spectra of iPP, nano-Lig, and nano-Lig/iPP composites are shown in Figure 1(b). The peaks from 2837 cm^{-1} to 2953 cm^{-1} and the peaks from 1375 cm^{-1} to 1454 cm^{-1} were assigned to stretching vibration and bending vibration of methylene of iPP, respectively. The wide peak from 1500 cm^{-1} to 1800 cm^{-1} was the stretching vibration of the aromatic ring skeleton of nano-Lig. A new wide peak from 1500 cm^{-1} to 1800 cm^{-1} was shown in all nano-Lig/iPP composites, which could be assigned to the characteristic peaks of the aromatic ring skeleton of nano-Lig. The results demonstrated that nano-Lig/iPP composites were prepared successfully.

3.2. Thermal Stability of Nano-Lig/iPP Composites. Figure 2 shows the TG curves of iPP, nano-Lig, and nano-Lig/iPP. The TG results of iPP, nano-Lig, and nano-Lig/iPP are shown in Table 1. For nano-Lig, a mass loss occurred at around 100°C, possibly because of water evaporation in nano-Lig. The T_d (the temperature at which the initial mass of the material has been lost) of nano-Lig was 210.0°C. For iPP, the T_d and T_i (the temperature at which 5 wt% of the initial mass of the material has been lost) of iPP were 354.8°C and 400.0°C, respectively. For nano-Lig/iPP composites, the T_d and T_i of nano-Lig/iPP composites were larger than those of iPP compared with iPP; furthermore, the T_d and T_i of nano-Lig/iPP composites increased with the increase of the nano-Lig content in nano-Lig/iPP composites, suggesting all nano-Lig/iPP composites had higher thermostability compared to iPP. The T_i of nano-Lig/iPP composite increased by 34.4°C when the nano-Lig content was 2 wt% in nano-Lig/iPP composites. While a previous report showed that T_i of lignin/iPP composite prepared by melt mixing lignin (not nano-Lignin) and iPP increased by 33°C when the lignin content was 5 wt% in lignin/iPP composites [49]. Also, another previous report showed that T_i of lignin/iPP composite decreased by 7°C under N_2 atmosphere and increased by 23°C when the lignin content was 5 wt% in lignin/iPP composites [52]. This result demonstrated that nano-Lig had a more effective promotion in the thermostability of iPP than lignin. These results indicated that nano-Lig could improve the thermostability of iPP.

3.3. Thermal Property of iPP and Nano-Lig/iPP Composites. Figures 3(a) and 3(b) show the DSC heating and cooling curves of iPP and nano-Lig/iPP composites, respectively. The DSC results data are listed in Table 2. The melting temperature (T_m) of the nano-Lig/iPP composites were comparable with that of iPP, while the melting enthalpy (ΔH) of the nano-Lig/iPP composites were higher than that of iPP. Thus, the crystallinity (X_c) of all nano-Lig/iPP composites were higher that of iPP. Compared with iPP, the highest X_c of nano-Lig/iPP composites increased by 6.39% when the nano-Lig content was 1 wt% in the nano-Lig/iPP composite. The crystallization temperature (T_c) of the nano-Lig/iPP composites shifted to a higher temperature compared to iPP. The results suggested that nano-Lig could serve as a nucleating agent for iPP because 1 wt% nano-Lig/iPP composite showed the highest X_c; thus, the characterization of 1 wt% nano-Lig/iPP composite are shown in the following parts.

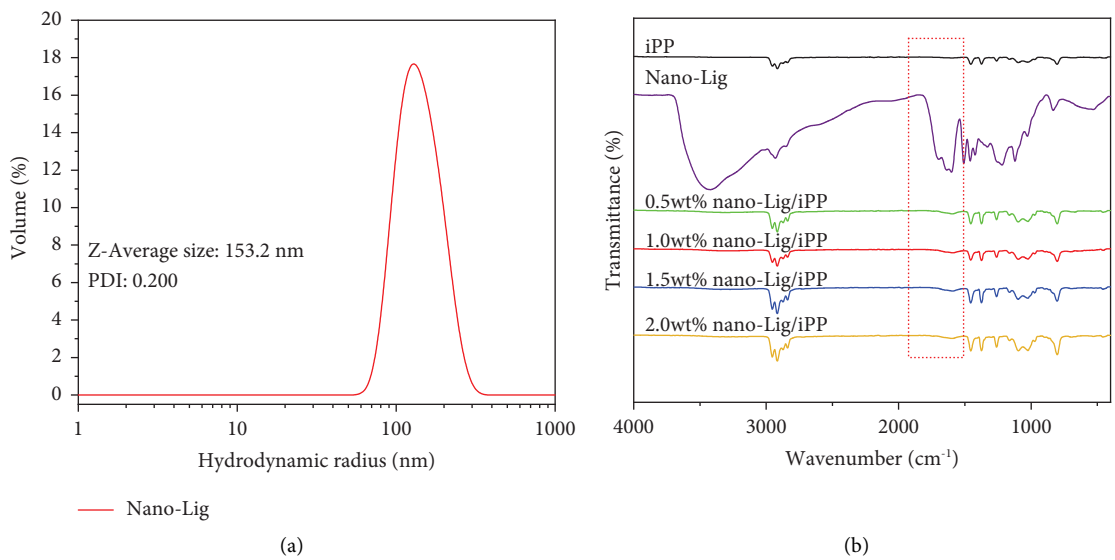

Figure 1: (a) Particle size distribution of nano-Lig in aqueous solution at room temperature. (b) FTIR Spectra of iPP, nano-Lig, and nano-Lig/iPP composites.

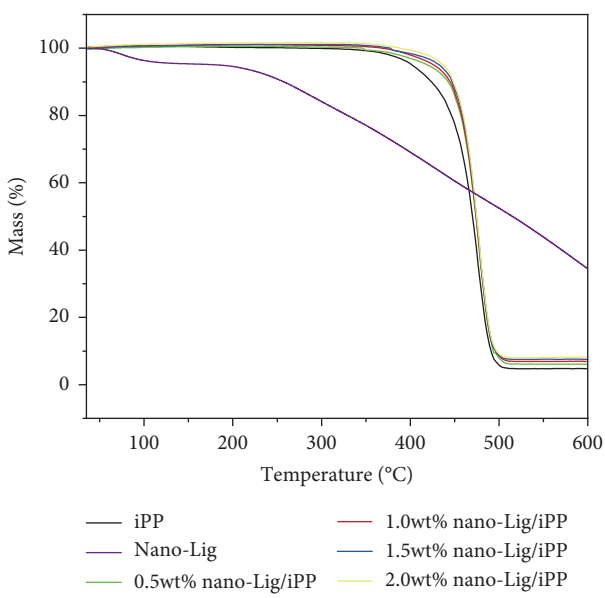

Figure 2: TG curves of iPP, nano-Lig, and nano-Lig/iPP composites.

3.3.1. Nonisothermal Crystallization Behavior of iPP and Nano-Lig/iPP Composites. Figure 4(a) shows the DSC crystallization curve of iPP at cooling rates of 2.5°C min^{-1}, 5.0°C min^{-1}, 10.0°C min^{-1}, and 20.0°C min^{-1}. The relative crystallinity (X_t) varying with temperature can be expressed by equation (2):

$$X_t = \frac{\Delta H_T}{\Delta H_\infty} = \frac{\int_{T_0}^{T} (dH_c/dT)dT}{\int_{T_0}^{T_\infty} (dH_c/dT)dT}, \quad (2)$$

where ΔH_∞ is the maximum enthalpy value reached at the end of the nonisothermal crystallization process and ΔH_T is the enthalpy evolved as a function of the crystallization temperature (T). T_0 and T_∞ represent the crystallization start and completion temperatures, respectively. Both H_∞ and ΔH_T can be acquired through the software of a standard DSC. Using equation (2), the relationship between X_t and crystallization temperature for iPP at different cooling rates can be obtained and is shown in Figure 4(b).

Table 1: TG results of iPP, nano-Lig, and nano-Lig/iPP composites.

Samples	T_d (°C)	T_i (°C)
iPP	354.8	400.0
Nano-Lig	210.0	—
0.5 wt% nano-Lig/iPP	364.5	418.2
1.0 wt% nano-Lig/iPP	385.3	425.3
1.5 wt% nano-Lig/iPP	388.0	430.5
2.0 wt% nano-Lig/iPP	405.2	434.4

The relationship between T and the crystallization time (t) is shown in equation (3), where R is the cooling rate.

$$t = \frac{(T_0 - T)}{R}. \quad (3)$$

By using equation (3), the relationship between X_t and T (Figure 4(b)) can be converted to the relationship between X_t and t for iPP (Figure 4(c)). Figure 4(d) shows the DSC crystallization curve of nano-Lig/iPP at cooling rates of 2.5°C min^{-1}, 5.0°C min^{-1}, 10.0°C min^{-1}, and 20.0°C min^{-1}. Figures 4(e) and 4(f) show the relationship between X_t and T and the relationship between X_t and t of nano-Lig/PP, respectively. When $X_t = 50\%$, the half time of crystallization ($t_{1/2}$) can be obtained from Figures 4(c) and 4(f). The value of the inverse of $t_{1/2}$ reflects the relative crystallization rate of iPP and nano-Lig/iPP, i.e., the smaller $t_{1/2}$ is, the larger the inverse of $t_{1/2}$ is and the faster relative crystallization rate is. The crystallization kinetic

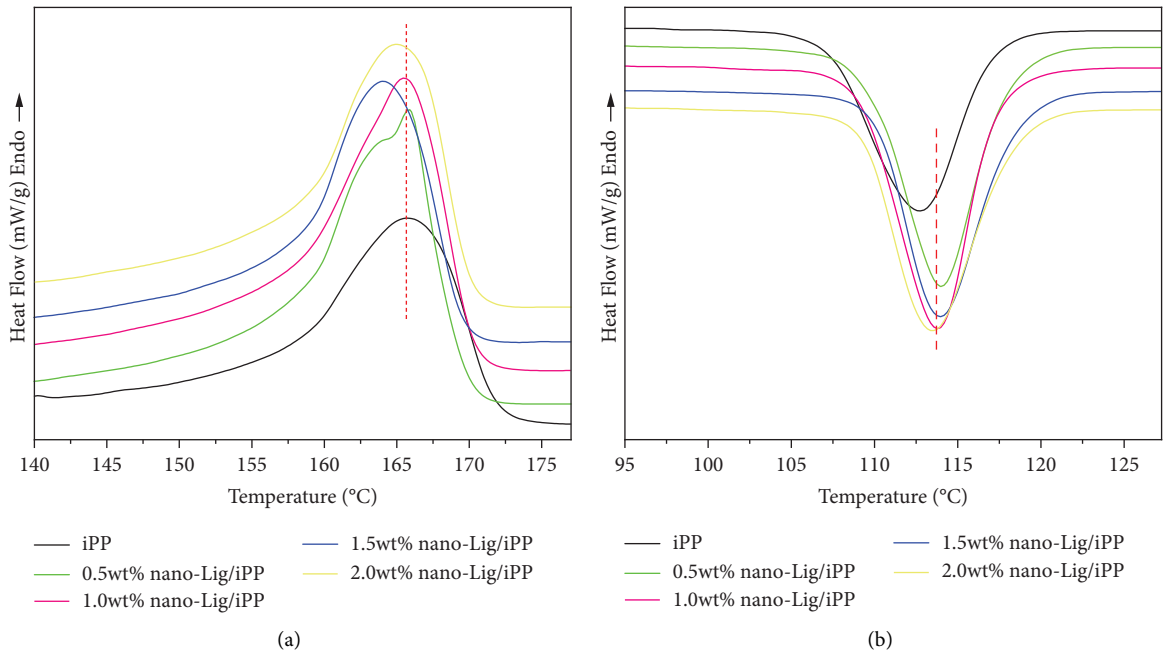

Figure 3: (a) and (b) are the DSC second heating curves and the DSC second cooling curves of iPP and nano-Lig/iPP composites, respectively.

Table 2: DSC results of iPP and nano-Lig/iPP composites.

Samples	T_m (°C)	ΔH (J·g^{-1})	X_c (%)	T_c (°C)
iPP	165.8	63.11	30.49	112.7
0.5 wt% nano-Lig/iPP	165.4	73.66	35.47	114.0
1.0 wt% nano-Lig/iPP	165.3	75.57	36.88	113.8
1.5 wt% nano-Lig/iPP	164.1	68.59	33.64	114.0
2.0 wt% nano-Lig/iPP	165.0	71.94	35.46	113.4

T_m is the melting temperature, ΔH is the melting enthalpy, and T_c is the crystallization temperature.

parameters of iPP and nano-Lig/iPP are obtained from Figure 4 and shown in Table 3. It was found that T_c of iPP and nano-Lig/iPP decreased with the increase of the cooling rate due to the thermal hysteresis phenomenon of iPP. At the same cooling rate, T_c of nano-Lig/iPP was higher than that of iPP, and $t_{1/2}$ of nano-Lig/iPP was smaller than that of iPP, suggesting that nano-Lig could promote the crystallization of iPP. The result is consistent with our expectation that a smaller amount of nano-Lig (only 1 wt%) can accelerate the crystallization kinetics because it acts as a nucleating agent. However, a previous report showed that lignin could promote iPP crystallization when the lignin content was 5 wt% in lignin/iPP composites [49].

3.3.2. Analysis of Dynamic Parameters of Avrami. Using the abovementioned X_t and t data, the isothermal crystallization of iPP and nano-Lig/iPP can be described by the modified Avrami equation (4) [53, 54].

$$X_t = 1 - e^{-Z_t (Rt)^n}, \quad (4)$$

where Z_t is the crystallization rate constant; R is the cooling rate; and n is the Avrami exponent. To obtain Z_t and n values, equations (4) can be converted to (5).

$$\lg\left[-\ln\left(1 - X_t\right)\right] = \lg Z_t + n\lg(Rt). \quad (5)$$

Figures 5(a) and 5(b) are the straight lines obtained by plotting $\lg[-\ln(1 - X_t)]$ versus $\lg(Rt)$ of iPP and nano-Lig/iPP, respectively. Values of n and Z_t were determined from the slope and the intercept of the straight lines in Figure 5, respectively, and shown in Table 4.

Z_t Values of iPP and nano-Lig/iPP were comparable at the same cooling rate, at the cooling rate of 10.0°C min^{-1} and 20.0°C min^{-1}, and the n values of both iPP and nano-Lig/iPP were larger than 3. At the cooling rate of 2.5°C min^{-1} and 5.0°C min^{-1}, the n values of nano-Lig/iPP were larger than 3 and the n values of iPP were smaller than 3. The results indicated the three-dimensional growth of iPP crystalline units is induced by heterogeneous nucleation.

3.4. X-Ray Diffraction Analysis. Figure 6 shows the XRD spectra of iPP and 1 wt% nano-Lig/iPP composite. iPP showed typical α-crystal diffraction peaks at $2\theta = 14.1°$, 16.8°, 18.5°, 21.1°, and 21.8°, which was related to (110), (040), (130), (131), and (111) crystalline planes, respectively [55–57]. The characteristic peaks of 1 wt% nano-Lig/iPP composite were similar to those of iPP, indicating that the nano-Lig's effects on the crystallization behavior of iPP were negligible, and the crystalline structure of iPP remained unchanged in the composite.

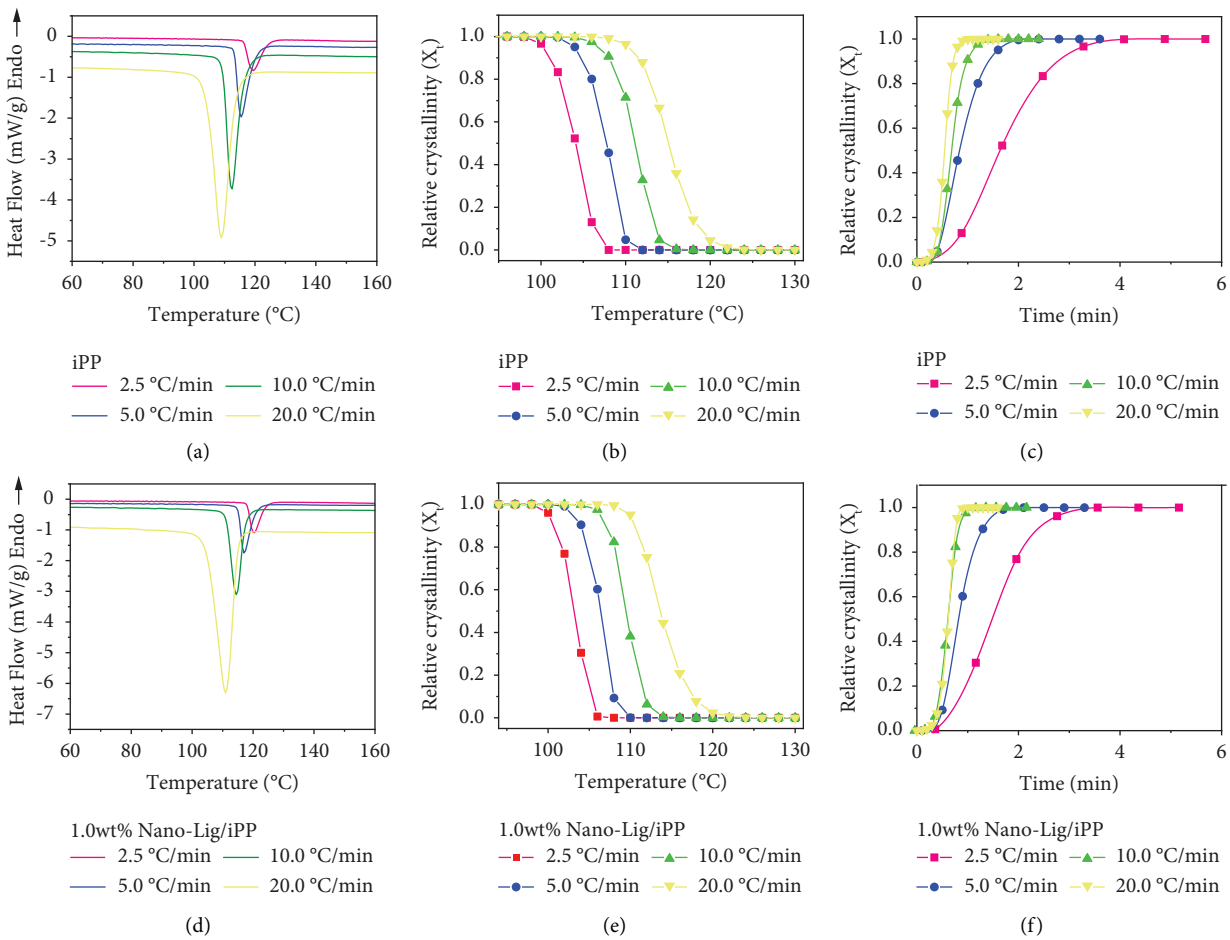

Figure 4: (a) and (d) are nonisothermal crystallization curves of iPP and nano-Lig/iPP at different cooling rates, respectively. (b) and (e) are relative crystallinity (X_t) verse temperature during the nonisothermal crystallization process at different cooling rates for iPP and nano-Lig/iPP, respectively. (c) and (f) are the relationship of X_t and time during the nonisothermal crystallization process at different cooling rates for iPP and nano-Lig/iPP, respectively.

Table 3: Nonisothermal crystallization kinetic parameters of iPP and nano-Lig/iPP.

Samples	Cooling rate (°C·min^{-1})	T_c (°C)	$t_{1/2}$ (s)
iPP	2.5	119.8	1.64
	5.0	117.9	0.85
	10.0	114.3	0.69
	20.0	109.0	0.54
Nano-Lig/iPP	2.5	121.2	1.48
	5.0	119.5	0.82
	10.0	115.2	0.62
	20.0	111.1	0.60

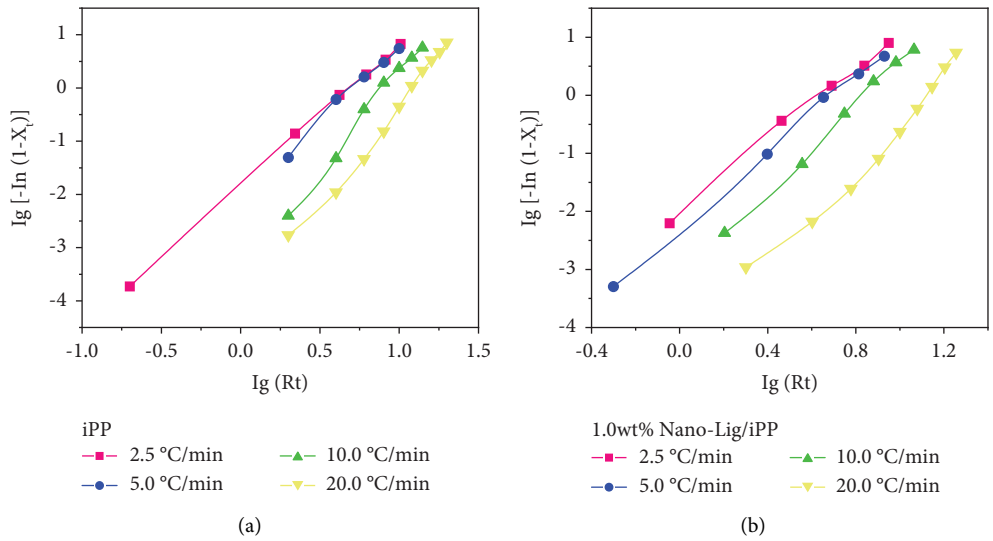

Figure 5: The relationship between $\lg[-\ln(1-X_t)]$ and $\lg(R(t))$ of (a) iPP and (b) nano-Lig/iPP at different cooling rates.

Table 4: Nonisothermal crystallization kinetic parameters of iPP and nano-Lig/iPP by the modified Avrami method.

Samples	Cooling rate (°C·min^{-1})	$Z_t \times 10^4$	n
iPP	2.5	145	2.66
	5.0	81.6	2.88
	10.0	2.96	3.85
	20.0	0.758	3.80
Nano-Lig/iPP	2.5	100	3.08
	5.0	51.7	3.27
	10.0	6.60	3.79
	20.0	0.353	3.96

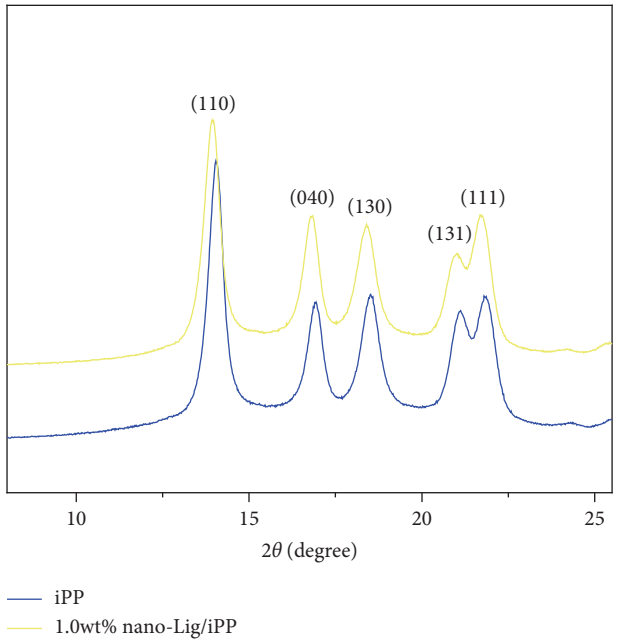

Figure 6: XRD curves of iPP and 1 wt% nano-Lig/iPP composite.

4. Conclusion

In this work, nano-Lignin (nano-Lig) was prepared successfully by the self-assembly method. Nano-Lig could improve thermostability and crystallization properties of iPP. The T_i of nano-Lig/iPP composite increased by 34.4°C when the nano-Lig content was 2 wt% in nano-Lig/iPP composites. The crystallinity of iPP increased by 6.39% when 1.0 wt% nano-Lig was added in iPP. The study of kinetics with nonisothermal crystallization found that nano-Lig can increase the crystallization rate of iPP.

Data Availability

The research data used to support the findings of this study are included within the article.

Conflicts of Interest

The authors declare that there are no conflicts of interest.

Authors' Contributions

Jing Chen conceptualized (lead), performed the methodology (lead) and writing original draft preparation (equal). Tao Yang performed data curation (equal), investigation (equal), and writing original draft preparation (equal). Yongchen Zhu performed data curation, investigation, and writing original draft preparation (equal). Zhenyang Luo supervised (lead) the study. Xiaofeng Ma performed review writing & editing (Lead) and supervised (lead) the study. The authors Jing Chen, Tao Yang, and Yongchen Zhu contributed equally.

Acknowledgments

This work was supported by the Priority Academic Program Development of Jiangsu Higher Education Institutions (PAPD).

References

[1] C. C. Hsu, P. H. Geil, H. Miyaji, and K. Asai, "Structure and properties of polypropylene crystallized from the glassy state," *Journal of Polymer Science Part B: Polymer Physics*, vol. 24, no. 10, pp. 2379–2401, 1986.

[2] M. L. Di Lorenzo and C. Silvestre, "Non-isothermal crystallization of polymers," *Progress in Polymer Science*, vol. 24, no. 6, pp. 917–950, 1999.

[3] Y. Mubarak, E. M. A. Harkin-Jones, P. J. Martin, and M. Ahmad, "Modeling of non-isothermal crystallization kinetics of isotactic polypropylene," *Polymer*, vol. 42, no. 7, pp. 3171–3182, 2001.

[4] L. Liu, Y. Zhao, C. Zhang, Z. Dong, K. Wang, and D. Wang, "Morphological characteristics of β-nucleating agents governing the formation of the crystalline structure of isotactic polypropylene," *Macromolecules*, vol. 54, no. 14, pp. 6824–6834, 2021.

[5] S. Qiu, Y. Zheng, A. Zeng, and Y. Guo, "Prediction of non-isothermal crystallization parameters for isotactic polypropylene," *Thermochimica Acta*, vol. 512, no. 1-2, pp. 28–33, 2011.

[6] M. Van Drongelen, T. B. Van Erp, and G. W. M. Peters, "Quantification of non-isothermal, multi-phase crystallization of isotactic polypropylene: the influence of cooling rate and pressure," *Polymer*, vol. 53, no. 21, pp. 4758–4769, 2012.

[7] S. F. Ran, X. H. Zong, D. F. Fang, B. S. Hsiao, B. Chu, and R. A. Phillips, "Structural and morphological studies of isotactic polypropylene fibers during heat/draw deformation by in-situ synchrotron SAXS/WAXD," *Macromolecules*, vol. 34, no. 8, pp. 2569–2578, 2001.

[8] I. L. Hosier, R. G. Alamo, and J. S. Lin, "Lamellar morphology of random metallocene propylene copolymers studied by atomic force microscopy," *Polymer*, vol. 45, no. 10, pp. 3441–3455, 2004.

[9] S. Brückner, S. V. Meille, V. Petraccone, and B. Pirozzi, "Polymorphism in isotactic polypropylene," *Progress in Polymer Science*, vol. 16, no. 2-3, pp. 361–404, 1991.

[10] R. A. Campbell, P. J. Phillips, and J. S. Lin, "The gamma phase of high-molecular-weight polypropylene: 1. Morphological aspects," *Polymer*, vol. 34, no. 23, pp. 4809–4816, 1993.

[11] D. Lyu, Y. Y. Sun, Y. Q. Lai et al., "Advantage of preserving Bi-orientation structure of isotactic polypropylene through die drawing," *Chinese Journal of Polymer Science*, vol. 39, no. 1, pp. 91–101, 2020.

[12] J. Kang, G. S. Weng, Z. F. Chen et al., "New understanding in the influence of melt structure and β-nucleating agents on the polymorphic behavior of isotactic polypropylene," *RSC Advances*, vol. 4, no. 56, pp. 29514–29526, 2014.

[13] S. Iwasaki, M. Inoue, Y. Takei, R. Nishikawa, and M. Yamaguchi, "Modulus enhancement of polypropylene by sorbitol nucleating agent in flow field," *Polym. Cryst.*vol. 4, no. 2, Article ID e10170, 2020.

[14] T. A. Shepard, C. R. Delsorbo, R. M. Louth et al., "Self-organization and polyolefin nucleation efficacy of 1,3:2,4-di-p-methylbenzylidene sorbitol," *Journal of Polymer Science Part B: Polymer Physics*, vol. 35, no. 16, pp. 2617–2628, 1997.

[15] T. Kobayashi, M. Takenaka, K. Saijo, and T. Hashimoto, "Self-assembly and morphology of gel networks in l,3:2,4-bis-o-(p-methylbenzylidene)-D-sorbitol/n-dibutylphthalate," *Journal of Colloid and Interface Science*, vol. 262, no. 2, pp. 456–465, 2003.

[16] M. Kristiansen, M. Werner, T. Tervoort, P. Smith, M. Blomenhofer, and H. W. Schmidt, "The binary system isotactic polypropylene/bis(3,4-dimethylbenzylidene)sorbitol: phase behavior, nucleation, and optical properties," *Macromolecules*, vol. 36, no. 14, pp. 5150–5156, 2003.

[17] T. Kobayashi and T. Hashimoto, "Development of self-assembling nucleators for highly transparent semi-crystalline polypropylene," *Bulletin of the Chemical Society of Japan*, vol. 78, no. 2, pp. 218–235, 2005.

[18] A. Nogales, G. R. Mitchell, and A. S. Vaughan, "Anisotropic crystallization in polypropylene induced by deformation of a nucleating agent network," *Macromolecules*, vol. 36, no. 13, pp. 4898–4906, 2003.

[19] L. Balzano, G. Portale, G. W. M. Peters, and S. Rastogi, "Thermoreversible DMDBS phase separation in iPP: the effects of flow on the morphology," *Macromolecules*, vol. 41, no. 14, pp. 5350–5355, 2008.

[20] J. Zhou and Z. Xin, "Relationship between molecular structure and nucleation of benzylidene acetals in isotactic polypropylene," *Polymer Composites*, vol. 33, no. 3, pp. 371–378, 2012.

[21] T. Bauer, R. Thomann, and R. Mülhaupt, "Two-component gelators and nucleating agents for polypropylene based upon supramolecular assembly," *Macromolecules*, vol. 31, no. 22, pp. 7651–7658, 1998.

[22] C. P. Martin, A. S. Vaughan, S. J. Sutton, and S. G. Swingler, "Crystallization behavior of a propylene/ethylene copolymer: nucleation and a clarifying additive," *Journal of Polymer Science Part B: Polymer Physics*, vol. 40, no. 19, pp. 2178–2189, 2002.

[23] Y. Zhao, A. S. Vaughan, S. J. Sutton, and S. G. Swingler, "On the crystallization, morphology and physical properties of a clarified propylene/ethylene copolymer," *Polymer*, vol. 42, no. 15, pp. 6587–6597, 2001.

[24] M. Tenma and M. Yamaguchi, "Structure and properties of injection-molded polypropylene with sorbitol-based clarifier," *Polymer Engineering & Science*, vol. 47, no. 9, pp. 1441–1446, 2007.

[25] J. X. Li and W. L. Cheung, "Pimelic acid-based nucleating agents for hexagonal crystalline Polypropylene," *Journal of Vinyl and Additive Technology*, vol. 3, no. 2, pp. 151–156, 1997.

[26] H. N. Beck, "Heterogeneous nucleating agents for polypropylene crystallization," *Journal of Applied Polymer Science*, vol. 11, no. 5, pp. 673–685, 1967.

[27] Y.-F. Zhang and J.-J. Mao, "Effect of chemical structure of hydrazide compounds on nucleation effect in isotactic polypropylene," *Journal of Polymer Research*, vol. 26, no. 12, p. 277, 2019.

[28] K. Yang, Q. Yang, G. Li, Y. Sun, and D. Feng, "Morphology and mechanical properties of polypropylene/calcium carbonate nanocomposites," *Materials Letters*, vol. 60, no. 6, pp. 805–809, 2006.

[29] K. Mitsuishi, S. Ueno, S. Kodama, and H. Kawasaki, "Crystallization behavior of polypropylene filled with surface-modified calcium carbonate," *Journal of Applied Polymer Science*, vol. 43, no. 11, pp. 2043–2049, 1991.

[30] P. McGenity, J. Hooper, C. Paynter et al., "Nucleation and crystallization of polypropylene by mineral fillers: relationship to impact strength," *Polymer*, vol. 33, no. 24, pp. 5215–5224, 1992.

[31] H. Zhao and R. K. Y. Li, "Crystallization, mechanical, and fracture behaviors of spherical alumina-filled polypropylene nanocomposites," *Journal of Polymer Science Part B: Polymer Physics*, vol. 43, no. 24, pp. 3652–3664, 2005.

[32] D. Libster, A. Aserin, and N. Garti, "Advanced nucleating agents for polypropylene," *Polymers for Advanced Technologies*, vol. 18, no. 9, pp. 685–695, 2007.

[33] F. Vásquez-Garay, I. Carrillo -Varela, C. Vidal, P. Reyes -Contreras, M. Faccini, and R. Teixeira Mendonça, "A review on the lignin biopolymer and its integration in the elaboration of sustainable materials," *Sustainability*, vol. 13, no. 5, p. 2697, 2021.

[34] A. Thumm, R. Risani, A. Dickson, and M. Sorieul, "Lignocellulosic fibre sized with nucleating agents promoting transcrystallinity in isotactic polypropylene composites," *Materials*, vol. 13, no. 5, p. 1259, 2020.

[35] Q. Tang, Y. Qian, D. Yang, X. Qiu, Y. Qin, and M. Zhou, "Lignin-based nanoparticles: a review on their preparations and applications," *Polymers*, vol. 12, no. 11, p. 2471, 2020.

[36] N. Zhou, W. P. D. W. Thilakarathna, and Q. He, "HPV. Rupasinghe, A review: depolymerization of lignin to generate high-value bio-products: opportunities, challenges, and prospects," *Frontiers in Energy Research*, vol. 9, Article ID 758744, 2022.

[37] D. Bajwa, G. Pourhashem, A. Ullah, and S. Bajwa, "A concise review of current lignin production, applications, products and their environmental impact," *Industrial Crops and Products*, vol. 139, Article ID 111526, 2019.

[38] V. K. Ponnusamy, D. D. Nguyen, J. Dharmaraja et al., "A review on lignin structure, pretreatments, fermentation reactions and biorefinery potential," *Bioresource Technology*, vol. 271, pp. 462–472, 2019.

[39] A. J. Ragauskas, G. T. Beckham, M. J. Biddy et al., "Lignin valorization: improving lignin processing in the biorefinery," *Science*, vol. 344, no. 6185, Article ID 1246843, 2014.

[40] Q. Q. Tang, M. S. Zhou, Y. X. Li, X. Q. Qiu, and D. J. Yang, "Formation of uniform colloidal spheres based on lignosulfonate, a renewable biomass resource recovered from pulping spent liquor," *ACS Sustainable Chemistry & Engineering*, vol. 6, no. 1, pp. 1379–1386, 2018.

[41] I. Haq, P. Mazumder, and A. S. Kalamdhad, "Recent advances in removal of lignin from paper industry wastewater and its industrial applications-A review," *Bioresource Technology*, vol. 312, Article ID 123636, 2020.

[42] T. C. Nirmale, B. B. Kale, and A. J. Varma, "A review on cellulose and lignin based binders and electrodes: small steps towards a sustainable lithium ion battery," *International Journal of Biological Macromolecules*, vol. 103, pp. 1032–1043, 2017.

[43] H. Mainka, O. Täger, E. Körner et al., "Lignin - an alternative precursor for sustainable and cost-effective automotive carbon fiber," *Journal of Materials Research and Technology*, vol. 4, no. 3, pp. 283–296, 2015.

[44] A. Cayla, F. Rault, S. Giraud, F. Salaün, V. Fierro, and A. J. P. Celzard, "PLA with intumescent system containing lignin and ammonium polyphosphate for flame retardant textile," *Polymers*, vol. 8, no. 9, p. 331, 2016.

[45] A. S. Hoffman, "Hydrogels for biomedical applications," *Advanced Drug Delivery Reviews*, vol. 64, pp. 18–23, 2012.

[46] P. Figueiredo, K. Lintinen, J. T. Hirvonen, M. A. Kostiainen, and H. A. Santos, "Properties and chemical modifications of lignin: towards lignin-based nanomaterials for biomedical applications," *Progress in Materials Science*, vol. 93, pp. 233–269, 2018.

[47] P. Mishra and R. Wimmer, "Aerosol assisted self-assembly as a route to synthesize solid and hollow spherical lignin colloids and its utilization in layer by layer deposition," *Ultrasonics Sonochemistry*, vol. 35, pp. 45–50, 2017.

[48] Z. Zhang, V. Terrasson, and E. Guénin, "Lignin nanoparticles and their nanocomposites," *Nanomaterials*, vol. 11, no. 5, p. 1336, 2021.

[49] M. Canetti, A. De Chirico, and G. Audisio, "Morphology, crystallization and melting properties of isotactic polypropylene blended with lignin," *Journal of Applied Polymer Science*, vol. 91, no. 3, pp. 1435–1442, 2004.

[50] M. Lievonen, J. J. Valle-Delgado, M.-L. Mattinen et al., "A simple process for lignin nanoparticle preparation," *Green Chemistry*, vol. 18, no. 5, pp. 1416–1422, 2016.

[51] C. Ruiz-Orta, J. P. Fernandez-Blazquez, A. M. Anderson-Wile, G. W. Coates, and R. G. Alamo, "Isotactic polypropylene with (3,1) chain-walking defects: characterization, crystallization, and melting behaviors," *Macromolecules*, vol. 44, no. 9, pp. 3436–3451, 2011.

[52] M. Canetti, F. Bertini, A. De Chirico, and G. Audisio, "Thermal degradation behaviour of isotactic polypropylene blended with lignin," *Polymer Degradation and Stability*, vol. 91, no. 3, pp. 494–498, 2006.

[53] A. Jeziorny, "Parameters characterizing the kinetics of the non-isothermal crystallization of poly(ethylene terephthalate) determined by d.s.c," *Polymer*, vol. 19, no. 10, pp. 1142–1144, 1978.

[54] A. K. Ahmed, M. Atiqullah, D. R. Pradhan, and M. A. Al-Harthi, "Crystallization and melting behavior of i-PP: a perspective from Flory's thermodynamic equilibrium theory and DSC experiment," *RSC Advances*, vol. 7, no. 67, pp. 42491–42504, 2017.

[55] L. Huang, Q. Wu, S. Li, R. Ou, and Q. Wang, "Toughness and crystallization enhancement in wood fiber-reinforced polypropylene composite through controlling matrix nucleation," *Journal of Materials Science*, vol. 53, no. 9, pp. 6542–6551, 2018.

[56] J. Yang, M. Gao, H. Zhao, S. Liu, M. Hu, and S. Xie, "Space charge characteristics of polypropylene modified by rare earth nucleating agent for β crystallization," *Materials*, vol. 12, no. 1, p. 42, 2018.

[57] C. Lv, S. Luo, and W. Guo, "Investigation of the crystallization and mechanical properties of wood fiber/polypropylene composites nucleated by a self-assemblyβ-nucleating agent," *Polymer Bulletin*, 2022.